ISSN (e) 2520-7393
ISSN (p) 2521-5027
www.estirj.com

# Effective Aluminum-Cobalt based Mixed Metal Oxide Nanocomposite for Water splitting

Rehan Ali Qureshi[1], Dr. Muhammad Ishaque Abro[2], Dr. Umair Aftab[3]

[1,2,3]*Department of Metallurgy and Materials Engineering Mehran University of Engineering and Technology Jamshoro Pakistan.*

**Abstract:** Renewable energy materials with better efficiency are in high demand for advanced applications. In this study, we report effective aluminum-cobalt based mixed metal oxide nanocomposite for oxygen evolution reaction application. The as synthesized nanocomposite offers better electrical conductivity and high density of oxygen vacancies. The prepared material also offers low overpotential of 321 mV at a current density of 20 mA/cm$^2$, with charge transfer resistance of 75 Ω. The results suggest that addition of $Co_2O_3$ into $Al_2O_3$, not only modified the morphology and also altered the interfacial chemistry of the material and could lead to better charge transfer at the interface during electrochemical applications.

**Keywords:** *Mixed Metal Oxide Nanocomposite, Water Splitting, Oxygen Evolution Reaction, Charge Transfer Resistance.*

## 1. Introduction

Reliance on fossil fuels have brought its reserves on the verge of depletion and the time is not so far when the world will be depriving of non-renewable resources of energy [1]. However, renewable energy sources are present but being transient in nature they have somewhat Cope present and future energy demands and are emerging and transitioning more towards uninterrupted forms [2]. Among the available alternative forms of energy, hydrogen seems promising and continuous for future endeavors [3]. Hydrogen energy, for being non-toxic and less pollutant, is gaining pivotal consideration in the energy sector. Its wide applications in batteries, aerospace technology, and hybrid and hydrogen powered vehicles are considered to bring a more positive impact on economy. More attention is also being drawn to establish hydrogen stations for hydrogen powered vehicles in the coming future [4]. Safe and economic hydrogen production was abstruse in past as most of hydrogen is available in the form of compounds of nitrogen, water, ammonia etc. [5, 6].

Hydrogen extraction from any of these sources require ample cost, and can only be obtained through mere electrolysis. Among these available sources for hydrogen production, water is available in a colossal volume. It Covers 71% of earth surface and is yet to be utilized for energy production [7, 8]. Water can be split into Hydrogen and Oxygen through electro-catalytic water splitting [9, 10]. The required benchmark voltage at which hydrogen is obtained is 0 volt which is possible through Platinum catalyst [11]. Platinum being the most expensive material cannot be utilized for industrial applications. But just recently through number of experiments the benchmark voltage is made possible through non-noble metal oxide based electrocatalysts [12]. Since research and experimental investigation on hydrogen from water has already reached application level therefore now there is a need to work in water oxidation [13]. There is still enough room available for the synthesis of stable and low over-potential electrocatalyst for water oxidation. Water Oxidation is a green and nonhazardous way to generate dioxygen from water [14]. Oxygen Evolution Reaction through electrochemical water splitting is another productive route of energy generation just like Hydrogen Evolution Reaction [15]. But oxygen obtained at higher over-potential is yet another apex to pare. Oxygen evolution reaction is a four electron thermodynamically sluggish process [16]. To obtain oxygen at a low over-potential is a constriction but not implausible[17]. Thriving to obtain an efficient low over-potential electrocatalyst with an optimum performance for OER is capitulating [18].

Presently, water oxidation through electrocatalysts is being achieved through non-precious metal chalcogenide, hydroxides, sulphide, phosphides, and so forth. But the performance of these non-precious metals is meager and insignificant for industrial applications but also their synthesis involves environm [19]. The electro-catalytic performance of noble metal-based compounds (IrO2/RuO2) are of peerless attributes and are considered benchmark to assess characteristics of their Counter peers' i.e., non-precious metals [20]. The hindrance associated with noble metal-based compounds is their scarcity and high cost that led scientists to develop low-cost electro-catalysts having low over-potential for practical applications[21].

Presently, $Co_3O_4$ has gained intense attention due to its stabile catalytic activity in alkaline media. But its unfavorable conductivity and insignificant active sites are needed to be abridged to enable its use for energy generation purposes[22]. Ample study and research have been being conducted on understanding the structural features of $Co_3O_4$. For instance, in a literature review cobalt palladium oxide nanostructure was prepared which not only shows significant OER active sites but also oxidizes water at low over-potential of 250 volts [23]. In this research work, defect sites were created in hybrid $Co_3O_4$ nanostructures using co-

Corresponding author Email address: *raqureshi78@gmail.com*

precipitation technique assisted by CA5E15 nanocomposite structures.

## 2. Experimental Section

### *2.1 Materials*

99.999% pure cobalt chloride hexahydrate, urea and alumina ultrafien powder were purchased from signa Aldrich, Pakistan. High analytical grade chemicals were used throughout the experiment without further purication and DI water was used.

### *2.2 Synthesis of Co2O3-Al2O3 nanocomposite structures*

Material was prepared using wet chemical method. 4.75 gram of cobalt chloride hexahydrate, and 1.2-gram urea were added into 200 ml of DI water. The solution was stirred for 15 minutes to obtain homogeneous solution of Co3O4-pristine. Three samples of same composition were prepared. In two of the samples, later, 5 milligram and 10 milligram of alumina was added to form CA5 and CA10. The precursor solutions contained in beakers were covered with aluminium foil and set inside the electric oven for 5 hours at 105o C. Once the growth solution was obtained, it was washed several times with DI water and then was dried. The dried solution contained hydroxide phase which was to be converted to oxide phase in the next step. The dried solutions were calcinated at 500o C for 5 hours to obtain oxide phase of cobalt and alumina.

### *2.3 Morphological and Structural Characterization*

PANanalytics X-ray diffractometer, model: Phillips, with operating parameters i.e., 45 kV, 45 mA and CuKa @ 1.541oA – radiation, was used for sample characterization and quantitative analysis was carried out using HighScore Plus to examine crystalline phase of the materials.

JEOL SEM, Mode: JSM-6308L was utilized to observe structural morphology of the samples with operating parameter i.e., 20kV.

FTIR, model: FTIR-perkinElmer Spectrum-2, was used to analyze nanocomposite interaction with operating parameters between 4000 and 400 $cm^{-1}$.

### *2.4 Electrochemical Measurements*

For the analysis of electrocatalytic activity of the nanocomposite structures, LSV, CV and EIS were carried out in 1 M KOH aqueous solution. The obtained nanostructured materials were dissolved in 1 ml of DI water with 50 µL of 5% of nafion and sonicated for 15 minutes for proper dissolution to prepare ink for glassy carbon electrode (GCE). Prior to disposition of ink on GCE, it was thoroughly cleaned and sonicated in methanol to obtain finished, shiny surface. After deposition of ink the ink was dried at room temperature. Zview (scriber associates, Inc.) and OriginPro 8 were used to examine LSV, CV and EIS data. All obtained potentials were converted to RHE equivalents.

### *2.5 Results and Discussions*

Diffraction pattern of Co3O4-Pristine and CA5 are shown in Fig. 1. The diffraction pattern of Co3O4-prisitine matched cubic Co3O4 phase (JCPDS card no. 01-078-1970). The diffraction peaks at two theta angle 31.179, 44.676, 38.435, 36.739, 59.175, 65.031 and 55.485 corresponds to planes (220), (222), (400), (311), (440), (511) and (422) respectively. The diffraction pattern of CA5 nanocomposite confirmed new phase formation of CoAl2O4 along with Co3O4. The new phase diffraction peaks are matched JCPDS card no. 01-070-0753 with cubic crystalline phase, and the two theta values 31.179, 44.676, 38.435, 36.739, 59.175, 65.031 and 55.485 corresponds to (220), (222), (400), (311), (440), (511) and (422) planes respectively. The coexistence of CoAl2O4 phase along with Co3O4 is resulting in crystal structure and can favor in electrocatalyst activity of the nanocomposite.

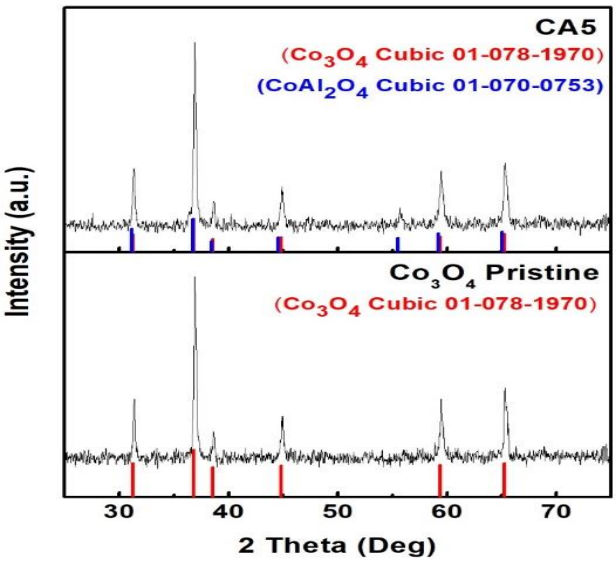


Fig. 1: XRD Diffraction pattern of Co3O4 – Pristine and CA5

Co3O4 and CA5 were examined by SEM characterization for assessment of morphological characteristics. The SEM micrographs of Co3O4 – Pristine and CA5 nanocomposites were shown in Fig. 2. The SEM micrograph of Co3O4 – Pristine revealed rod like morphology as seen in Fig. 2(a). While the CA5 nanocomposites exhibits the nano-spherical clusters of CoAl2O4 integrated with matrix of nano rod morphology of Co3O4 as illustrated in Fig. 2 (b).

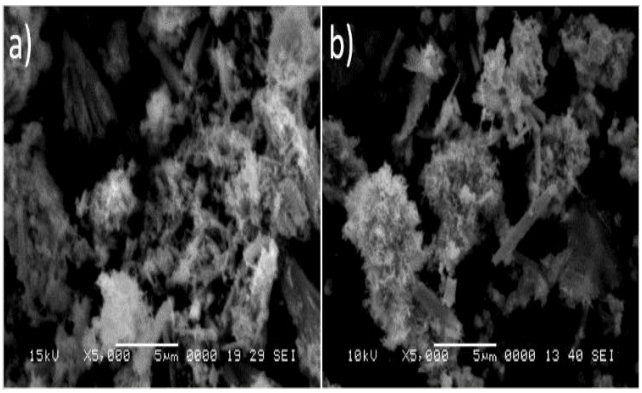


Fig. 2: SEM (a) Co3O4 - pristine (b) CA5

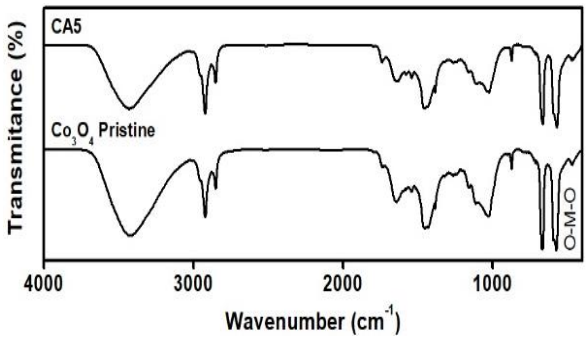


Fig. 3: FTIR of Co3O4 and CA5

FTIR analysis of prepared samples including Co3O4-Pristine and CA5 were performed for analysis of absorption bands and their corresponding groups as shown in Fig. 3. The FTIR spectra of Co3O4-Pristine represented the groups such as C-H, O-H, C-O, C=O and C=C at 2927 cm-1, 3438 cm-1, 1035 cm-1, 1797 cm-1 and 878 cm-1. In addition, the metal oxide peaks at 663 and 570 cm-1 of Co-O and O-Co-O confirms the formation of cobalt oxide. However, the spectrum of CA5 resembles with cobalt oxide peaks such as C-H, O-H, C-O, C=O and C=C, but the minor difference can be examined in metal oxide peaks of M-O which validates the presence of CoAl2O4.

### *2.6 Electrochemistry of OER*

The synthesized samples' electrochemistry was analyzed by linear sweep voltammetry (LSV) in 1 M KOH solution. The LSV polarization curves of Co3O4 – Pristine and CA5 given in Fig. 4 (a). The overpotential of CA5 was the lowest i.e., 310 mV vs RHE, whereas the overpotential of CA10 and pristine Co3O4 was 332 mV and 355 mV respectively at 20 mA/cm2 current density. The tafel slope values of pristine Co3O4, CA5 and CA10 are found to be 102 mV/dec, 75 mV/dec and 91 mV/dec as shown in Fig. 4 (b). Tafel slope values demonstrate the reaction kinetics taking place for applicable OER activity and are mentioned in Table 1. Pristine Co3O4 possess the highest tafel value of 102 mV/dec while CA5 has the lowest value of 75 mV/dec as compared to CA10 with a tafel value of 91.6. The tafel value of CA5 suggested that Step 3 is the rate limiting in this study. Therefore, the formation of CoAl2O4-Co3O4 nanocomposite is favorable for OER activity.

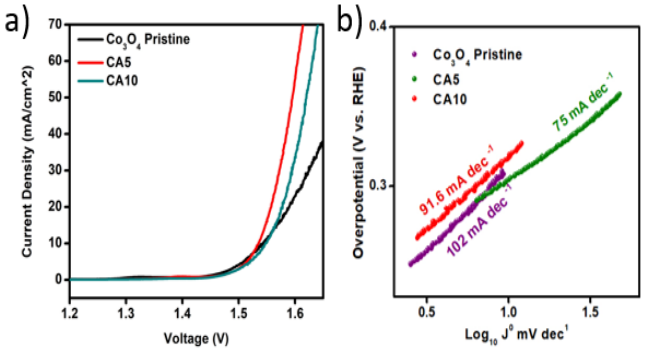


Fig. 4 (a) LSV Polarization curves of as synthesized nanocomposites (b) Tafel slopes

Table 1: The reaction kinetics of ER in alkaline media

| Steps | Reaction Kinetics | Tafel Slope |
|---|---|---|
| (1) | M + OH- → MOH + e- | 15 |
| (2) | MOH + OH- → MO- +H2O | 40 |
| (3) | MO- → MO + e- | 60 |
| (4) | 2MO → 2M + O2 + 2e- | 120 |

The EIS method was used to evaluate the charge transfer resistance at the electrode electrolyte interface in 1 M KOH as shown in Fig. 5. The EIS data was analyzed by using Z view software, equivalent circuit is shown in Fig. 5 and its values are reported in Table 2. The charge transfer resistances (Rct) of $Co_3O_4$-Pristine, CA5 and CA10 are found to be 478 Ω, 221 Ω and 343 Ω respectively. The lower charge transfer resistance of CA5 is the reason of accelerated charge transfer between the electrode and electrolyte interface and confirmed an enhanced OER activity.

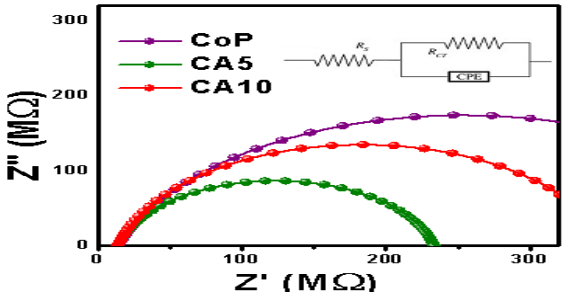


Fig. 5: Nyquist plot of as synthesized nanocomposites in 1M KOH at potentials of 10 mV in the frequency range of 100 kHz to 0.1 Hz

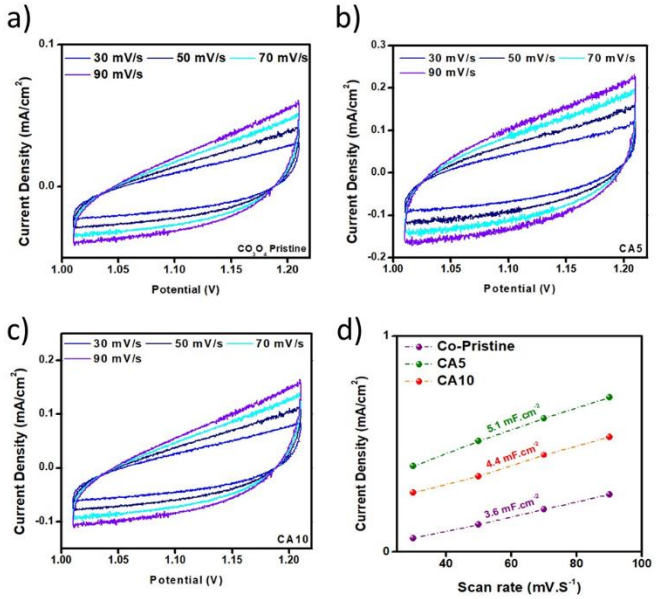


Fig. 6: CV curves at various scan rates for the determination of double layer capacitance of (a) Co3O4-pristine & (b) CA5 (c) CA10 (d) Current densities vs scan rates

Table 2: Summarizes the distinguishing characteristics of the current OER Catalyst.

| Catalyst | Tafel Slope (mV/dec) | Charge Resistance (Ω) | Double Layer Capacitance (μF/cm2) | ECSA (cm2) |
|---|---|---|---|---|
| Co3O4–pristine | 102 | 478 | 3.6 | 90 |
| CA5 | 75 | 221 | 5.1 | 127.5 |
| CA10 | 91 | 343 | 4.4 | 110 |

For the determination of electrochemical double layer capacitance (Cdl) and electrochemical active surface area (ESCA) , cyclic voltammetry was employed as shown in Fig. 6 (a-c). The current density vs scan rate slopes were determined using CV curves and shown in Fig. 6 (d). Slopes of these curves is the electrochemical double layer capacitance (Cdl) and ECSA was obtained from Cdl to assess effective active sites.

$$\text{ECSA} = \frac{C_{dl}}{C_s}$$

Where Cs is the specific capacitance of the electrolyte used (0.04 for KOH). The Cdl and ECSA values are shown in Table 2. It reveals that the CA5 has the greater ECSA value which proves that there was a significant improvement in the OER activity due to actives sites within nanocomposite.

## 3. Conclusions

In this experimental study, CA5 nanocomposite were generated through wet chemical method. SEM technique assured changes in the morphology of the nanocomposite structures. The SEM characterization illustrated nearly the same structures with some sharp nano-rods like structure due to deposition of Co3O4 onto Alumina. The XRD also assured the addition of Co3O4 into Alumina thereby increasing the lattice parameter. A durability test for 30 hours also showed no significant changes in the performance of the CA5 nanocomposite structure but also remained nearly unchanged during the durability test. The EIS confirmed the charge transfer resistance of 80 ohms which is pivotal for OER functioning of the material.
The findings suggest that doping of Co3O4 into alumina to synthesize CA5 is of crucial importance to develop materials for OER with significantly low overpotential for energy generation applications.

## References


1. Żywiołek, J.R.-S.J.K.M.A.A.U.S.A.T.i.R.E.a.P.o.E.-S.K. *Trust in Renewable Energy as Part of Energy-Saving Knowledge*

Energies, 2022. **15**, DOI: 10.3390/en15041566.

2. Tabandeh, A., M.J. Hossain, and L. Li, *Integrated multi-stage and multi-zone distribution network expansion planning with renewable energy sources and hydrogen refuelling stations for fuel cell vehicles.* Applied Energy, 2022. **319**: p. 119242.
3. Huang, W., J. Dai, and L. Xiong, *Towards a sustainable energy future: Factors affecting solar-hydrogen energy production in China.* Sustainable Energy Technologies and Assessments, 2022. **52**: p. 102059.
4. Wang, L., et al., *Two-way dynamic pricing mechanism of hydrogen filling stations in electric-hydrogen coupling system enhanced by blockchain.* Energy, 2022. **239**: p. 122194.
5. Ali, I., et al., *Role of the radiations in water splitting for hydrogen generation.* Sustainable Energy Technologies and Assessments, 2022. **51**: p. 101926.
6. Gong, Y., et al., *Perspective of hydrogen energy and recent progress in electrocatalytic water splitting.* Chinese Journal of Chemical Engineering, 2022. **43**: p. 282-296.
7. Hoseinzadeh, S. and D. Astiaso Garcia, *Techno-economic assessment of hybrid energy flexibility systems for islands' decarbonization: A case study in Italy.* Sustainable Energy Technologies and Assessments, 2022. **51**: p. 101929.
8. Okunlola, A., et al., *Techno-economic assessment of low-carbon hydrogen export from Western Canada to Eastern Canada, the USA, the Asia-Pacific, and Europe.* International Journal of Hydrogen Energy, 2022. **47**(10): p. 6453-6477.
9. Aftab, U., et al., *Two step synthesis of TiO2–Co3O4 composite for efficient oxygen evolution reaction.* International Journal of Hydrogen Energy, 2021. **46**(13): p. 9110-9122.
10. Bhatti, A.L., et al., *An Efficient and Functional Fe3O4/Co3O4 Composite for Oxygen Evolution Reaction.* Journal of Nanoscience and Nanotechnology, 2021. **21**(4): p. 2675-2680.
11. Han, W., et al., *Cobalt-Based Metal-Organic Frameworks and Their Derivatives for Hydrogen Evolution Reaction.* Frontiers in Chemistry, 2020. **8**(1025).
12. Meng, Y.-L., et al., *Hierarchical MoO42– Intercalating α-Co(OH)2 Nanosheet Assemblies: Green Synthesis and Ultrafast Reconstruction for Boosting Electrochemical Oxygen Evolution.* Energy & Fuels, 2021. **35**(3): p. 2775-2784.
13. Wu, Y., R. Sun, and J. Cen, *Facile Synthesis of Cobalt Oxide as an Efficient Electrocatalyst for Hydrogen Evolution Reaction.* Frontiers in Chemistry, 2020. **8**(386).
14. Zhang, J.-Y., et al., *Local spin-state tuning of cobalt–iron selenide nanoframes for the boosted oxygen evolution.* Energy & Environmental Science, 2021. **14**(1): p. 365-373.
15. Aftab, U., et al., *Mixed CoS2@Co3O4 composite material: An efficient nonprecious electrocatalyst for hydrogen evolution reaction.* International Journal of Hydrogen Energy, 2020. **45**(27): p. 13805-13813.
16. Guo, Q., et al., *Reducing Oxygen Evolution Reaction Overpotential in Cobalt-Based Electrocatalysts via Optimizing the "Microparticles-in-Spider Web" Electrode Configurations.* Small, 2020. **16**(8): p. 1907029.
17. Concina, I., Z.H. Ibupoto, and A. Vomiero, *Semiconducting Metal Oxide Nanostructures for Water Splitting and Photovoltaics.* Advanced Energy Materials, 2017. **7**(23): p. 1700706.
18. Liu, M., et al., *Palladium as a Superior Cocatalyst to Platinum for Hydrogen Evolution Using Covalent Triazine Frameworks as a Support.* ACS Applied Materials & Interfaces, 2020. **12**(11): p. 12774-12782.
19. Katkar, P.K., et al., *Synthesis of hydrous cobalt phosphate electro-catalysts by a facile hydrothermal method for enhanced oxygen evolution reaction: effect of urea variation.* CrystEngComm, 2019. **21**(5): p. 884-893.

20. Hirakawa, K., M. Inoue, and T. Abe, *Methanol oxidation on carbon-supported Pt–Ru and TiO2 (Pt–Ru/TiO2/C) electrocatalyst prepared using polygonal barrel-sputtering method*. Electrochimica Acta, 2010. **55**(20): p. 5874-5880.

21. Liu, X., et al., *Noble metal–metal oxide nanohybrids with tailored nanostructures for efficient solar energy conversion, photocatalysis and environmental remediation*. Energy & Environmental Science, 2017. **10**(2): p. 402-434.

22. Polat, O., et al., *Engineering the band gap of LaCrO3 doping with transition metals (Co, Pd, and Ir).* Journal of Materials Science, 2018. **53**(5): p. 3544-3556.

23. Gong, L., et al., *Enhanced Catalysis of the Electrochemical Oxygen Evolution Reaction by Iron(III) Ions Adsorbed on Amorphous Cobalt Oxide.* ACS Catalysis, 2018. **8**(2): p. 807-814.